Science of the Total Environment 800 (2021) 149561

Contents lists available at ScienceDirect

Science of the Total Environment

journal homepage: www.elsevier.com/locate/scitotenv

Optimization of the phototrophic Cyanobacteria polyhydroxybutyrate (PHB) production by kinetic model simulation

Estel Rueda [a], Joan García [b,*]

[a] GEMMA-Group of Environmental Engineering and Microbiology, Department of Civil and Environmental Engineering, Escola d'Enginyeria de Barcelona Est (EEBE), Universitat Politècnica de Catalunya-BarcelonaTech, Av. Eduard Maristany 16, Building C5.1, E-08019 Barcelona, Spain
[b] GEMMA-Group of Environmental Engineering and Microbiology, Department of Civil and Environmental Engineering, Universitat Politècnica de Catalunya-BarcelonaTech, c/ Jordi Girona 1-3, Building D1, E-08034 Barcelona, Spain

HIGHLIGHTS

- New model for photosynthetic PHB production was successfully calibrated ($r^2 > 0.6$).
- According to model, PHB production was more affected by cell lysis and N inhibition.
- Optimal cultivation conditions should be modified according to environmental factors.
- 6.4 $mgN \cdot L^{-1}$ and 2 $mgP \cdot L^{-1}$ were the optimum nutrients for batch PHB production.
- PHB productivity of 5 $mg \cdot L^{-1} \cdot d^{-1}$ was achieved with new reactor configuration.

GRAPHICAL ABSTRACT

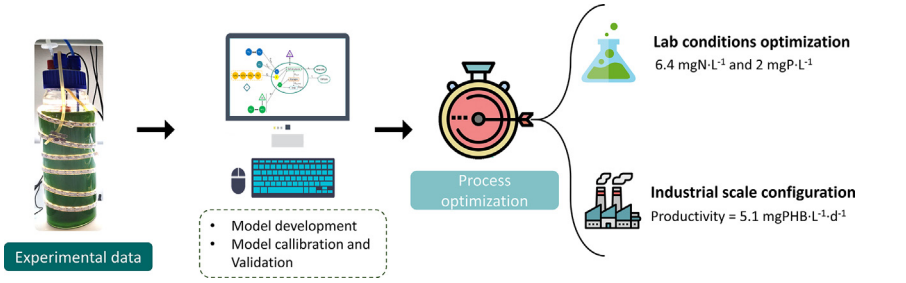

ARTICLE INFO

Article history:
Received 21 June 2021
Received in revised form 5 August 2021
Accepted 6 August 2021
Available online 12 August 2021

Editor: Damia Barcelo

Keywords:
Microalgae
Mathematical model
Synechocystis
Polyhydroxyalkanoates (PHAs)
Glycogen
Bioplastics

ABSTRACT

Cyanobacteria can grow using inorganic substrates, such as CO_2 from industrial sources and nutrients from wastewaters, and therefore are promising microorganisms to produce polyhydroxybutyrate in a cleaner circular context. However, this biotechnological production is highly challenging because it involves different interlinked reactions that are affected by environmental conditions, which hinders process optimization. In this study a new biokinetic mechanistic model using novel experimental approaches was developed to optimize polyhydroxybutyrate (PHB) and glycogen production. The model includes, for the first time, the production of glycogen and its conversion into PHB, which has been found as the main pathway to produce PHB. Model was successfully (r^2: 0.6–0.99) calibrated and validated with experimental data from photobioreactors inoculated with *Synechocystis* sp. The developed model was used to determine suitable initial conditions for a lab scale batch reactor (6.4 $mgN \cdot L^{-1}$ and 2 $mgP \cdot L^{-1}$) and a new configuration for the continuous industrial production of PHB was proposed and optimized using this tool. The maximum productivity (5.1 $mgPHB \cdot L^{-1} \cdot d^{-1}$) and the optimal configuration and operation of the serial reactors to produce PHB in an industrial scale was achieved using a hydraulic retention time of 4 days in the growth reactor. Then, this reactor daily fed 20 batch accumulation reactors, which were discharged after 20 days. The optimal influent nutrients concentrations for this configuration was found to be 50 $mgN \cdot L^{-1}$ and 10 $mgP \cdot L^{-1}$. Results found in this study show the necessity to optimize biopolymers production with Cyanobacteria considering environmental conditions, and demonstrated the potential of this model as a tool to increase PHB productivity.

* Corresponding author at: c/ Jordi Girona 1-3, Building D1, E-08034 Barcelona, Spain.
E-mail address: joan.garcia@upc.edu (J. García).

https://doi.org/10.1016/j.scitotenv.2021.149561

1. Introduction

Accumulation of non-biodegradable plastics in the environment is of worldwide concern. To fight this problem, new restrictions banning the use of plastics are appearing. Indeed, in 2018, the European commission banned several plastic products (Carpine et al., 2020). Disposal of these plastics is also complicated, as they are barely degraded in landfills, incineration produce toxic by-products and recycling is time consuming and changes polymer properties, which hinders their further utilization (Carpine et al., 2020). An alternative material to beat these problems is the use of bioplastics. Polyhydroxybutyrate (PHB) is one of the most promising commercially produced bioplastics, whose production is expected to quadruple in the following years (Zhang et al., 2019). However, its production costs are still high compared to petroleum-based polymers (Costa et al., 2019). Cyanobacteria are of particular interest as PHB producers, because of their capacity to grow using inorganic substrates that could come from wastewater (Arias et al., 2020) and to mitigate CO_2 emissions (Abed et al., 2009; Zhang et al., 2019). Process optimization is not trivial because phototrophic PHB production involves different metabolic interlinked pathways which are regulated by multiple environmental factors (Arias et al., 2018; Drosg et al., 2015). PHB are accumulated in Cyanobacteria only during nutrients (N and/or P) limitation periods. In these conditions, Cyanobacteria redirect the excess of carbon to internal carbon reserve polymers, such as glycogen and PHB. Therefore, PHB production is usually done in two-steps; first, they grow in nutrients replete medium and second, they are exposed to nutrient limitation. Between those two steps, biomass separation is required to replace the medium by a nutrient limited one (Drosg et al., 2015; Kamravamanesh et al., 2019). At full scale operations, this intermediate separation might considerably increase the production costs, which will hinder scalation of the process. Therefore, establishing a self-limiting one-step cultivation process is essential to reach an efficient process (Drosg et al., 2015; Kamravamanesh et al., 2019). To do that, enough nutrients should be provided for the cells to grow, and at the same time, cells should have finished these nutrients when they reach the stationary growth phase. The amount of nutrients that should be provided is not universal; it depends on several environmental factors, such as light and reactor design.

Mathematical models can be useful tools for process optimization and to increase process efficiency. There are several models on PHB production with heterotrophic organisms (Carucci et al., 2001; Gujer et al., 1999; Kaelin et al., 2009; Lai et al., 2013; Mulchandani et al., 1989). However, only one deals with phototrophic accumulation of PHB with the strain *Synechocystis* PCC6803 (Carpine et al., 2018). This model assumes two types of cells: growing cells and PHB producing cells. Cell growth was modelled following the Droop formulation (Droop, 1973), while nutrients uptake were simulated by a Monod type kinetic. The formation rate of PHB producing cells depended on the initial nitrate concentration, and the PHB production rate was described as a linear relation with the CO_2 concentration. pH and temperature effects were not considered in this model, as well as the glycogen accumulation and conversion to PHB, which has been recently demonstrated to be the major source of carbon for PHB production in Cyanobacteria (Dutt and Srivastava, 2018; Kamravamanesh et al., 2018; Koch et al., 2019).

In the present study, recent research advances were included in a new improved kinetic model for bioplastics production with Cyanobacteria. This model includes for the first time, the process of glycogen synthesis and further conversion to PHB. Following the idea proposed by Ryu et al. (2018), the proposed model considers that cells are composed by 3 essential components: active biomass, PHB and glycogen. Active biomass can grow using inorganic carbon, but also using the internal carbon storage compounds (i.e. PHB and glycogen). On the other side, PHB and glycogen can be generated by uptaking the excess of inorganic carbon, and additionally PHB can also be formed from glycogen conversion. Similar to previous models (Carpine et al., 2018; Ryu et al., 2018), macronutrients (NO_3^-, NH_4^+, PO_4^{3-} and inorganic C) assimilation and utilization rates were consumed following a Droop equation. However, in the present model, in contrast with the model by Carpine et al. (2018), NH_4^+ utilization was also included. This property allows our model to predict Cyanobacteria growth and PHB production, not only using BG-11 growth media, but also with other cultivation media containing ammonia as nitrogen source. The effect of significant environmental factors, which were not considered in previous models, such as temperature and pH, were also included (see Table S1 for model comparison with previous models).

Experimental data for model calibration and validation were obtained from 3 L photobioreactors with *Synechocystis* sp. monoculture. Parameter sensitivity analysis was also carried out with the aim to assess the most relevant parameters on biomass, PHB and glycogen production. Eventually, the calibrated model was used for process optimization in two different scenarios: 1) to optimize initial N and P concentrations to maximize the PHB productivity in the 3 L reactors. 2) to assess the best operation strategy and nutrients supply of a proposed configuration to produce PHB at an industrial scale. The overall aim of this work is to create a reliable tool, that will help to optimize the PHB and glycogen production process with Cyanobacteria considering the light and nutrients availability and reactor design.

2. Materials and methods

2.1. Model description

2.1.1. Conceptual model

Fig. 1 shows a general schematic representation of the model, which is made up by 14 processes describing nutrients uptake, Cyanobacteria growth, lysis and endogenous respiration, PHB production, glycogen production, conversion of glycogen to PHB and gas transfer to the air.

Cyanobacteria can grow using dissolved inorganic carbon (DIC), glycogen (Gly) or PHB. To grow on DIC cells need to receive light. On the other hand, light is not needed for cells to grow on Glycogen or PHB, although, these reactions are inhibited by the presence of inorganic carbon. Cells can only uptake inorganic carbon in the form of CO_2 and bicarbonate (HCO_3^-) (Markou et al., 2014). Finally, biomass lysis releases cell internal components (PHB, glycogen, and cell structures) to the medium generating NH_4^+, CO_2 and P. Additionally, inorganic carbon excess can be stored as glycogen and PHB, which will be a readily available source of carbon when DIC is not available. Photosynthetic synthesis of PHB and glycogen can only occur when there is an unbalance in nitrogen and phosphorus. Eventually, as suggested by many authors (Dutt and Srivastava, 2018; Kamravamanesh et al., 2018; Koch et al., 2019; Rueda et al., 2020a), PHB can be synthetized by the degradation of glycogen. Dissolved oxygen and CO_2 are gradually transferred from the culture to the air. As a result of Cyanobacteria photosynthesis, protons (H^+) are consumed, resulting in a pH increase. This increase produces a change in the chemical equilibriums of inorganic carbon and phosphorus species.

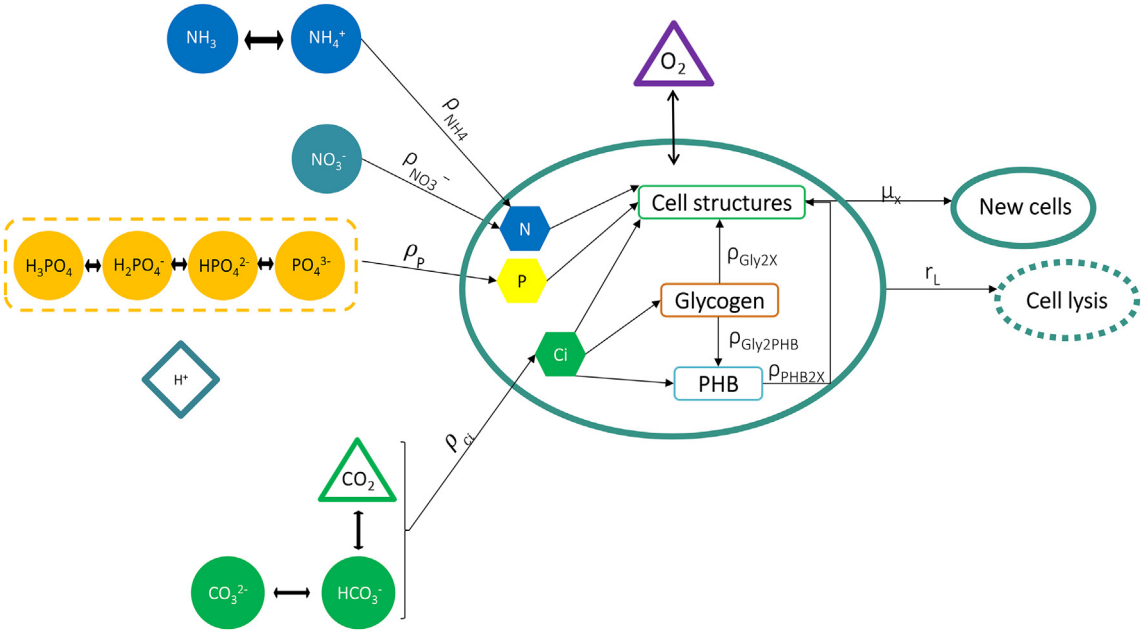

Fig. 1. General simplified schematic representation of the conceptual model showing the main processes and species considered. Arrows represent processes. Species in triangles are gases and the ones inside circles are soluble species.

2.1.2. Model processes

The structure of this model was inspired on previous Activated Sludge Models (ASM) (Gujer et al., 1999). Detailed mathematical description of the processes can be found in Table 1. Process parameters and stoichiometric coefficients used in the model equations are listed in Supplementary materials Tables S3 and S6 respectively.

Mathematical expressions used in this study are based in the Droop model which allows predicting the growth under substrate limitation (Zhang et al., 2015). In the Droop model the intracellular concentration of nutrients is based on a nutrient quota (Q), which is defined as the mass ratio between nutrients and biomass (Zhang et al., 2015).

pH and temperature are also considered. Following the work by Solimeno et al., 2019 cardinal equations for pH and temperature are included to represent the inhibitory effects of growing at not optimal pH and temperature (Eqs. (1) and (2)). pH_{min}, T_{min} and pH_{max} and T_{max} represent the lower

Table 1
Mathematical description of model processes.

Process	No.	Rate
Cyanobacteria growth		
Cyanobacteria growth on Ci	1	$\rho_1 = \varphi(pH)\cdot\varphi(T)\cdot\mu_{xm}\cdot\left(\frac{Q_N}{q_{N,\,max}}\right)\cdot\left(\frac{Q_P}{q_{P,\,max}}\right)\cdot\left(\frac{Q_{Ci}}{q_{Ci,\,max}}\right)\cdot\frac{Iav}{K_{SI}+Iav}\cdot X$
Cyanobacteria growth on glycogen	2	$\rho_2 = \varphi(pH)\cdot\varphi(T)\cdot\mu_{xm}\cdot\left(1-\frac{Q_{Ci}}{q_{Ci,\,max}}\right)\cdot\left(\frac{Q_N}{q_{N,\,max}}\right)\cdot\left(\frac{Q_P}{q_{P,\,max}}\right)\cdot\frac{\%gly}{K_{gly}+\%gly}\cdot X$
Cyanobacteria growth on PHB	3	$\rho_3 = \varphi(pH)\cdot\varphi(T)\cdot\mu_{xm}\cdot\left(1-\frac{Q_{Ci}}{q_{Ci,\,max}}\right)\cdot\left(\frac{Q_N}{q_{N,\,max}}\right)\cdot\left(\frac{Q_P}{q_{P,\,max}}\right)\cdot\frac{\%PHB}{K_{PHB}+PHB}\cdot X$
Lysis	4	$\rho_4 = k_{lysis}\cdot X^2$
Endogenous respiration	5	$\rho_5 = k_{resp}\cdot\frac{[O_2]}{[O_2]+K_{O2}}\cdot X$
Nutrients uptake		
Ammonia uptake	6	$\rho_6 = \varphi(pH)\cdot\varphi(T)\cdot k_{NH4}\cdot\frac{[NH_4^+]}{K_N+[NH_4^+]}\cdot\left(1-\frac{Q_N}{q_{N,\,max}}\right)\cdot X$
Nitrate uptake	7	$\rho_7 = \varphi(pH)\cdot\varphi(T)\cdot k_{NO3}\cdot\frac{[NO_3^-]}{[NO_3^-]+K_N}\cdot\frac{K_{IN}}{K_{IN}+[NH_4^+]}\cdot\left(1-\frac{Q_N}{q_{N,\,max}}\right)\cdot X$
Phosphate uptake	8	$\rho_8 = \varphi(pH)\cdot\varphi(T)\cdot k_{PO4}\cdot\frac{[PO_4^{3-}]}{[PO_4^{3-}]+K_{PO_4^{3-}}}\cdot\left(1-\frac{Q_P}{q_{P,\,max}}\right)\cdot X$
IC uptake	9	$\rho_9 = \varphi(pH)\cdot\varphi(T)\cdot k_{IC}\cdot\frac{[CO_2]+[HCO_3^-]}{[CO_2]+[HCO_3^-]+K_{Ci}}\cdot\left(1-\frac{Q_{Ci}}{q_{Ci,\,max}}\right)\cdot X$
PHB and glycogen accumulation		
Glycogen production	10	$\rho_{10} = \varphi(pH)\cdot\varphi(T)\cdot k_{C2Gly}\cdot\frac{K_{IN}^{Gly}}{Q_N+K_{IN}^{Gly}}\cdot\frac{K_{IP}^{Gly}}{Q_P+K_{IP}^{Gly}}\cdot\left(\frac{Q_{Ci}}{q_{Ci,\,max}}\right)\cdot\left(1-\frac{\%gly}{gly_{max}}\right)\cdot X$
PHB production	11	$\rho_{11} = \varphi(pH)\cdot\varphi(T)\cdot k_{C2PHB}\cdot\frac{K_{IN}^{PHB}}{Q_N+K_{IN}^{PHB}}\cdot\frac{K_{IP}^{PHB}}{Q_P+K_{IP}^{PHB}}\cdot\left(\frac{Q_{Ci}}{q_{Ci,\,max}}\right)\cdot\left(1-\frac{\%PHB}{PHB_{max}}\right)\cdot X$
Glycogen conversion to PHB	12	$\rho_{12} = \varphi(pH)\cdot\varphi(T)\cdot k_{Gly2PHB}\cdot\frac{K_{IN}^{PHB}}{Q_N+K_{IN}^{Gly}}\cdot\frac{K_{IP}^{PHB}}{Q_P+K_{IP}^{Gly}}\cdot\frac{[gly]}{K_{gly}+[gly]}\cdot X$
Gas transfer to air		
CO_2 transfer to the air	13	$\rho_{20} = K_a^{CO2}\cdot(CO_2^{WAT}-[CO_2])$
O_2 transfer to the air	14	$\rho_{21} = K_a^{O2}\cdot(O_2^{WAT}-[O_2])$

and higher limits for pH and temperature at which Cyanobacteria can grow. Outside of this range all processes rates are 0. On the other hand, cardinal function becomes maximum at pH_{opt} and T_{opt}.

$$\varphi(pH) = \frac{(pH - pH_{max}) \cdot (pH - pH_{min})^2}{(pH_{opt} - pH_{min}) \cdot \left[(pH_{opt} - pH_{min}) \cdot (pH - pH_{opt}) - (pH_{opt} - pH_{max}) \cdot (pH_{opt} + pH_{min} - 2pH) \right]} \quad (1)$$

$$\varphi(T) = \frac{(T - T_{i,\,max}) \cdot (T - T_{i,\,min})^2}{(T_{opt} - T_{min}) \cdot \left[(T_{opt} - T_{min}) \cdot (T - T_{opt}) - (T_{opt} - T_{max}) \cdot (T_{opt} + T_{min} - 2T) \right]} \quad (2)$$

- *Cyanobacteria growth* (process 1–3, Table 1): Cyanobacteria can grow using three different carbon substrates; inorganic carbon (process 1), glycogen (process 2) and PHB (process 3). Cyanobacteria growth is also influenced by other parameters, such as nutrients concentrations and light. Factors influencing Cyanobacterial growth are multiplied by the maximum specific velocity to obtain the actual growing velocity.

$$\mu = \mu_{max} \cdot f(Q_N) \cdot f(Q_P) \cdot f(Q_C) \cdot f(I) \quad (3)$$

The effect of nutrients (N, P, C) $f(Q_i)$ on cell growth is expressed by the modified Droop model. Similarly to what was done by Ryu et al., 2018 the $f(Q_i)$ factor was calculated as:

$$f(Q_i) = \frac{Q_i}{q_{i,\,max}} \quad (4)$$

where Q_i ($g_i \cdot gX^{-1}$) is the actual quota, defined as the intracellular concentration of nutrient "i" divided by the biomass concentration. And $q_{i,\,max}$ ($g_i \cdot gX^{-1}$) is the maximum quota obtained at maximum growth.

When there is not inorganic carbon available, Cyanobacteria grow using PHB and glycogen. This growth velocity depends on glycogen and PHB content. Their effect is defined by a Monod-type equation (Table 1).

Eventually, cells need light to grow using inorganic carbon. Similarly to what was done by Carpine et al., 2018, the effect of light is defined by a Monod type equation (Eq. (5)).

$$f(I) = \frac{Iav}{K_{SI} + Iav} \quad (5)$$

where I_{av} in μmol photons $\cdot m^{-2} \cdot s^{-1}$ is the average light intensity and K_{SI} in μmol photons $\cdot m^{-2} \cdot s^{-1}$ is the half saturation constant of light intensity. I_{av} can be estimated in a simplified way by the Lambert-Beer law for light distribution (Eq. (6)).

$$I_{av} = \frac{I_0}{\sigma \cdot L \cdot X} \cdot (1 - e^{-\sigma \cdot L \cdot X}) \quad (6)$$

where I_0 is the incident light intensity in μmol photons $\cdot m^{-2} \cdot s^{-1}$, σ in $m^2 \cdot g^{-1}$ is the extinction coefficient and L the culture depth. In this case L is the reactor radius and σ is assumed to be 0.37 $m^2 \cdot g^{-1}$ (Carpine et al., 2018).

- *Cyanobacteria lysis* (process 4, Table 1): Similar to what was done by Zhang et al., 2015, Cyanobacteria decay follows a second order reaction with respect to biomass concentration. Decay is, thus, proportional to a specific velocity lysis coefficient (k_{lysis}) and to the square of cell concentration (Zhang et al., 2015). Lysis releases cell components to the environment in form of ammonia, phosphorus, DIC and inert particulate matter (X_I).
- *Cyanobacteria endogenous respiration* (process 5, Table 1): this process is modelled by a specific respiration coefficient (k_{resp}) and a Monod factor which considers the oxygen as a limiting factor. Endogenous respiration produces CO_2 and inert particulate matter (X_I).
- *Nutrients uptake* (process 6–9, Table 1): These processes were described by Monod type equations, where the maximum uptake rates are downregulated by the corresponding internal quota (Bougaran et al., 2010). Ammonium and nitrate are both considered in this model, although, ammonium is preferred by microalgae (Markou et al., 2014). To represent this, an inhibitory term is introduced in nitrate uptake (process 7, Table 1).
- *Photosynthetic production of PHB and glycogen* (process 10–11, Table 1): PHB and glycogen production rates are proportional to $f(Q_{IC})$ and to a specific production rate constant. Moreover, PHB and glycogen production are downregulated by the presence of nitrogen and phosphorus (Arias et al., 2018; Kamravamanesh et al., 2019). To represent this, similarly to what was done by Bekirogullari et al., 2018, inhibition factors for N and P are used.
- *Conversion of glycogen to PHB* (process 12, Table 1): This process is proportional to the conversion rate constant, and it is considered that until there is not enough glycogen accumulated in the cell, this process is not occurring. To represent this, a Monod type kinetic is used.
- *Gas transference to air* (process 13–14, Table 1): The transfer of CO_2 and O_2 to the air and conversely are based in the Henry's law:

$$\rho_i = K_{a,i} \cdot \left(S_i^{WAT} - S_i \right) \quad (7)$$

where i is the chemical species (CO_2 or O_2). S_i^{WAT} is the saturation concentration of gas in water in $g \cdot m^{-3}$. $K_{a,\,i}$ is the overall mass transfer coefficient of the gas in d^{-1} and S_i is the actual concentration in $g \cdot m^{-3}$.

- *Chemical Equilibrium and pH:* Acid-based equilibria are considered in order to predict the pH of the system and the different nutrient species in the medium. The pH prediction was done by expressing the concentrations of all ionic species in solution as a function of the H^+ concentration and the equilibrium constants. Doing so, a nonlinear equation with H^+ as the only unknown was obtained.

To solve the set of differential equations of this model, first this nonlinear equation, should be solved to calculate the H^+ concentration. Then, the dissociation equilibriums are corrected and the pH is calculated. This pH value is the input of the next time step to solve the ODEs (ordinary differential equations). More details about the pH model can be found in Supplementary materials (Eqs. (1)–(4) and Table S9).

2.1.3. Model components

1. Active Biomass, X ($gX \cdot m^{-3}$): Part of the biomass which is responsible for metabolic activity and cell division. The sum of active biomass, PHB and glycogen are the volatile suspended solids (VSS).
2. Ammonium, NH_4^+ ($gN \cdot m^{-3}$): The culture medium used for our experiments (BG-11) has no ammonium, however, it can be produced through endogenous respiration and Cyanobacteria lysis.
3. Nitrate, NO_3^- ($gN \cdot m^{-3}$): Nitrate is assimilated by Cyanobacteria during the regeneration of intracellular nitrogen quota.
4. Phosphorus, P_{tot} ($gP \cdot m^{-3}$): Phosphorus is the sum of all the different chemical species involved (H_3PO_4, $H_2PO_4^-$, HPO_4^{2-}, PO_4^{3-}). The relative proportion of these species change with pH. Organic phosphorus is not considered in this model.
5. Inorganic carbon, DIC ($gC \cdot m^{-3}$): Different inorganic carbon species (CO_2, HCO_3^-, CO_3^{2-}), which change in concentration depending on chemical equilibria. Inorganic carbon is assimilated by Cyanobacteria only as CO_2 and/or HCO_3^-. DIC is produced through endogenous respiration and Cyanobacteria lysis, and can be transferred to/from the air.
6. Oxygen, O_2 ($gO_2 \cdot m^{-3}$): Concentration of oxygen in water. Oxygen is produced or consumed in almost all the processes (except ammonia uptake and CO_2 transfer to the air). Its consumption or production is calculated from continuity equations as done in Dosta Parras (2007).
7. Nitrogen quota, Q_N ($gN \cdot gX^{-1}$): intracellular nitrogen quota is a term described in the Droop model (Droop, 1973) that represents the substrate stored per unit of Cyanobacteria active biomass. This nutrient quota may be further available for cell growth, even after nutrients dissolved in the growth media are depleted.
8. Phosphorus quota, Q_P ($gP \cdot gX^{-1}$): intracellular phosphorus is the ratio of internal phosphorus per unit of Cyanobacteria active biomass.
9. Carbon quota, Q_C ($gC \cdot gX^{-1}$): intracellular carbon is the ratio of internal carbon per unit of Cyanobacteria active biomass.
10. Glycogen, Gly ($gGlucose \cdot m^{-3}$): Glycogen is a carbon reserve in Cyanobacteria cells. It can be synthetized from inorganic carbon and is used as a carbon source for biomass growth and PHB synthesis. It is also degraded by cell lysis and endogenous respiration. The glycogen content is calculated as:

$$\%Gly = \frac{[Gly]}{[VSS]} \cdot 100 \tag{8}$$

11. Polyhydroxybutyrate, PHB ($gPHB \cdot m^{-3}$): PHB is another carbon storage compound. It can be synthetized from inorganic carbon and from glycogen. It is used as a carbon source for biomass growth. However, due to the interrupted tricarboxylic acid cycle of Cyanobacteria, PHB cannot be used as efficiently as glycogen (Drosg et al., 2015). PHB can also be degraded by cell lysis and endogenous respiration. The PHB content is calculated as follows:

$$\%PHB = \frac{[PHB]}{[VSS]} \cdot 100 \tag{9}$$

12. Inert particulate matter, X_I ($gTSS \cdot m^{-3}$): Inert particulate matter is generated by biomass lysis and endogenous respiration (Gujer et al., 1999; Solimeno et al., 2017), and therefore includes dead cells and other organic detritus.

2.1.4. Stoichiometric and parameter values

Stoichiometric matrix and parameter values used in this model are presented in Tables S2 and S5 in Supplementary Materials. Mathematical expression of each of the stoichiometric is shown in Table S7 in Supplementary Materials. From this information the reaction rate of each component can be calculated as follows (Eq. (10)):

$$r_i = \sum_{i=1}^{ni} \sum_{j=1}^{nj} \nu_{i,j} \cdot \rho_j \tag{10}$$

where i is the number of model component and j the number of process. ρ_j is the reaction rate in $mg \cdot L^{-1} \cdot d^{-1}$ and $\nu_{i,j}$ the stoichiometric coefficient (Solimeno et al., 2017). Moreover, for each process the continuity equation must be fulfilled. Eq. (11) shows the general expression of the continuity equation for a process j and an element c.

$$\sum_{i=1}^{ni} \sum_{j=1}^{nj} \nu_{i,j} \cdot i_{c,i} = 0 \tag{11}$$

where $\nu_{i,j}$ is the stoichiometric coefficient for component i and process j, and $i_{c,i}$ is the conversion factor of a component i to its elemental elements (C, N, P, O) (Table S8) (Dosta Parras, 2007).

2.2. Model calibration and sensitivity analysis

The model described in the previous section was implemented in COMSOL Multiphysics™ v.5.4. A 0-Dimension interface and the Reaction Engineering module with a semi-batch reactor were used to represent the experimental reactor.

The model was calibrated using authors' previously published data (see Table S10 and Fig. S2) (Rueda et al., 2020a). In these cultures, a monoculture of *Synechocystis* sp., was grown in column photobioreactors made of polymethacrylate with a diameter of 11 cm and a working volume of 2.5 L (Table 2). Three different culturing phases with different DIC concentrations were applied in this reactor (growing phase, a feast and famine phase and a feast phase). These experiments were done in duplicate.

27 parameters from the 48 parameters implemented in the model were calibrated, and the rest were obtained from previous studies as indicated in Table S3. Calibration procedure was done as follows (Brun et al., 2002); first, in order to assess which parameters had a greater influence on the model, a sensitivity analysis was done. To do this, the mean square root (msqr) of the sensitivity function for each model variable was calculated as follows (Eq. (12)):

$$\delta_j^{msqr} = \sqrt{\frac{1}{N}\cdot\sum_{i=1}^{ni}\sum_{j=1}^{nj}\left(\frac{\theta_{i,j}^{+20\%}-\theta_{i,j}^{-20\%}}{2\cdot\Delta p}\right)^2} \tag{12}$$

where $\theta_{i,j}^{+20\%}$ and $\theta_{i,j}^{-20\%}$ in $mg\cdot L^{-1}$, are the simulation results for a particular variable of interest (j) at a time i, when the value of the parameter p increased or decreased a 20%. Δp is the change produced in each parameter, in this case, a 20% of the parameter's values, and N is the number of values considered.

Parameters with higher sensitivity were calibrated by tuning its value and comparing the simulation results with the experimental data set. For each of the tried values and for each of the parameters calibrated, the squared correlation coefficient (r^2) (Eq. (13)) and the normalized root mean square error (NRMSQE) (Eq. (14)) were calculated to assess the accuracy of the calibration. The values of the parameters were chosen to minimize the NRSQE and maximize r^2. NRSQE and r^2 are calculated as:

$$r^2 = 1-\frac{\sum_{i=1}^{ni}\sum_{j=1}^{nj}\left(y_{i,j}-\theta_{i,j}\right)^2}{\sum_{i=1}^{ni}\sum_{j=1}^{nj}\left(y_{i,j}-\overline{y}_j\right)^2} \tag{13}$$

$$\mathrm{NRMSE} = \frac{\sqrt{\sum_{i=1}^{ni}\sum_{j=1}^{nj}\frac{\left(y_{i,j}-\theta_{i,j}\right)^2}{N}}}{\overline{y}} \tag{14}$$

where $\theta_{i,j}$ in $mg\cdot L^{-1}$ represents the values of the model for a particular variable of interest (j). $y_{i,j}$ in $mg\cdot L^{-1}$ is the experimental value of a particular variable of interest (j) at a particular experimental time (i). $\overline{y}_j$ in $mg\cdot L^{-1}$ is the mean value of the experimental data. And N is the number of experimental values.

Eventually, once the model was calibrated, the endpoint sensitivity analysis was carried out to assess the soundness of the model. Similarly to what was done by Carpine et al., 2018, the impact on cell concentration, PHB and glycogen at the endpoint (45 days) for a modification of a ±20% in the model parameters was determined. Hence, the endpoint sensitivity for each parameter can be calculated as:

$$\delta_p^{+20\%} = \frac{\theta_{end,j}^{+20\%}-\theta_{end,j}}{\theta_{end,j}}\cdot 100 \tag{15}$$

$$\delta_p^{-20\%} = \frac{\theta_{end,j}^{-20\%}-\theta_{end,j}}{\theta_{end,j}}\cdot 100 \tag{16}$$

where $\delta_p^{+20\%}$ and $\delta_p^{-20\%}$ in % are the sensitivity of a parameter p when this parameter was increased or decreased a 20% respectively. $\theta_{end,j}^{+20\%}$ and $\theta_{end,j}^{-20\%}$ in $mg\cdot L^{-1}$ are the result of the model at the endpoint (45 days) for a particular variable of interest (j), which can be PHB, glycogen or VSS, when the studied parameter is increased or decreased a 20% respectively. $\theta_{end,j}$ is the model value at endpoint (45 days) for a particular variable of interest (j), when no changes are done over any of the parameters. This methodology was used to present the sensitivity results, since it is really simple and understandable.

Table 2
Photobioreactor (PBR) characteristics, culturing conditions and culture medium composition of the datasets used for calibration (Cal) and validation (Val-1 and Val-2).

Data set	PBR characteristics					Initial conditions						Ref
	PBR volume (L)	Culture radius (cm)	Light intensity ($\mu molPAR\cdot m^{-2}\cdot s^{-1}$)	pH control	Agitation	NO_3^- ($mgN\cdot L^{-1}$)	P ($mgP\cdot L^{-1}$)	DIC ($mgC\cdot L^{-1}$)	Q_P	Q_N	Q_C	
Cal	2.5	5.5	37 (15 $h\cdot d^{-1}$)	Yes (HCl + CO_2)	Magnetic stirrer	63[a]	4.9	121[b]	0.0046	0.099	0.58	(Rueda et al., 2020a)
Val-1	3	5.75	102 (15 $h\cdot d^{-1}$)	Yes (HCl)	Magnetic stirrer	122	7[c]	272	0.007	0.11	0.23	This study
Val-2	3	5.75	102 (15 $h\cdot d^{-1}$)	Yes (HCl + CO_2)	Magnetic stirrer	108	4.8	118[d]	0.009	0.14	0.34	This study

[a] 10 $mgN\cdot L^{-1}$ were supplemented at day 20.
[b] Added in a feast-famine regime from day 31 to 38 and maintained at 120 $mgC\cdot L^{-1}$ afterwards.
[c] Addition of 6 $mgP\cdot L^{-1}$ at day 4 and 1 $mgP\cdot L^{-1}$ at day 10.
[d] Maintained at 120 $mgC\cdot L^{-1}$ after day 29.

2.3. Model validation

Data for model validation were obtained from duplicate experiments conducted ad hoc for the purposes of this study. Two different data sets (with duplicate reactors in each) were used from a monoculture of *Synechocystis* sp. in a 3 L column photobioreactors, with a radius of 5.75 cm. Light was provided with cool white LEDs placed at a distance of 20 cm from the reactor and warm white LED strips rolled up around the reactor. This illumination provided an average light intensity of 102 μmol PAR·m^{-2}·s^{-1} during 15 h per day. In the first data set, pH was regulated with HCl additions. In the second data set CO_2 injections were used to control the pH until day 10. From day 10 to 29 HCl was used to control the pH in order to reduce the concentration of DIC. Experimental results can be found in Tables S11 and S12.

The first data set was used to validate nutrient consumption and growth rate, while the second data set was used to validate PHB (Table 2).

2.4. Model applications

Two cases of study were used to determine optimal operation conditions to maximize PHB production. The first case study was conducted to determine the optimal initial concentration of nutrients (N and P) to attain a one step cultivation and improve PHB productivity in a batch lab scale reactor. Optimal conditions were determined for a column photobioreactor with a radius of 5.75 cm and illuminated with a light intensity of 102 μmol PAR·m^{-2}·s^{-1}. In this case, pH was controlled by means of CO_2 additions and DIC concentration was kept constant. To determine the optimal concentrations of nutrients several combinations of initial N and P were tried. For each combination PHB productivity at every time step was calculated and the maximum productivity was selected. Afterwards, the maximum productivity of each combination was compared to determine which combination had the best productivity.

In the second case study, the continuous production of PHB was optimized. Nutrient limitation is one of the most important factors to produce a high amount of PHB. Therefore, to produce PHB in a continuous way, the best strategy is to use reactors in series. In the first reactor Cyanobacteria are grown and nutrients are consumed. Then, the outflow of the first reactor is fed to a second semi-batch reactor were PHB and glycogen are accumulated. After certain hydraulic retention time (HRT_2) the second reactor is discharged. The outflow of the first reactor should be fed every day to a different accumulation tank in order to allow the culture reach nutrients limitation and thus, the accumulation of the biopolymers. In order to have a continuous production of PHB several accumulation reactors should be used (N° of accumulation reactors = HRT_2). The volume needed for each of the accumulation reactors is equal to the amount discharged in 1 day from the growing tank:

$$V_2 = \dot{Q}_1 \left(L \cdot d^{-1}\right) \cdot 1\ day \tag{17}$$

where V_2 is the volume of each of the accumulation reactors, Q_1 is the outlet flowrate of the growth reactor. Fig. 2 shows and schematic representation of the proposed configuration for the continuous production of PHB.

In this second case study, the best concentration of nutrients in the influent and the optimal hydraulic retention times (HRT_1 and HRT_2) of the growth and accumulation reactors to maximize the system productivity were determined for a column photobioreactors with a radius of 5.75 cm. The light was considered to be solar irradiation in Barcelona (Spain) in August (https://re.jrc.ec.europa.eu/pvg_tools/es/#DR). In this case study, pH was controlled by means of CO_2 additions and DIC concentration was kept constant at 120 mgC·L^{-1}. To determine the optimal operation conditions to maximize PHB productivity, several N and P inlet concentrations and several HRT_1 and HRT_2 were tried. For each combination, PHB productivity was calculated as follows:

$$Productivity = \frac{PHB_2^{OUT} \cdot \dot{Q}_1}{V_1 + V_2 \cdot N°accumulation\ tanks} \tag{18}$$

where PHB_2^{OUT} is the PHB in mg·L^{-1} concentration in the outlet of the accumulation reactor. $\dot{Q}_1$ in L·d^{-1} is the volumetric flow rate and V_1 and V_2 in L are the volume of the growth reactor and the volume of each accumulation reactor respectively.

2.5. Analytical methods

Samples from photobioreactors were periodically analyzed for biomass, nutrients and PHB and glycogen content. pH was continuously measured online in each PBR, by an online sensor (HI1001, HANNA instruments, Italy) placed inside the reactor. pH was kept at an optimum level (7–9) by the action of a pH controller (HI 8711, HANNA instruments, Italy), which activated a peristaltic pump or an electro valve to add HCl or CO_2 respectively.

DIC was measured by a C/N analyzer (C/N analyzer 2005, Analytikjena, Germany). NO_3^- and PO_4^{3-} were measured by the colorimetric methods described in Standard Methods (methodologies 4500-$NO3^-$ and 4500-PE) (APHA et al., 2012). Soluble alkalinity M and P were measured by a photometric kit from Lovibond (Tintometer, Amesbury, UK). Alkalinity was related to DIC with the following equation:

$$\mathrm{DIC}\left(\mathrm{mg}\cdot\mathrm{L}^{-1}\right) = \mathrm{H_2CO_3}\left(\mathrm{mg}\cdot\mathrm{L}^{-1}\right) + \mathrm{HCO_3}^{-}\left(\mathrm{mg}\cdot\mathrm{L}^{-1}\right) + \mathrm{CO_3}^{-2}\left(\mathrm{mg}\cdot\mathrm{L}^{-1}\right) = \mathrm{Alkalinity{-}M{-}Alkalinity{-}P} \tag{19}$$

To measure the soluble components, samples were filtrated through a 1–3 μm pore glass microfiber filter. Total suspended solids (TSS) and volatile suspended solids (VSS) were measured following the gravimetric methods described in Standard Methods (methodology 2540 D) (APHA et al., 2012).

To analyze PHB and glycogen, samples were frozen at −80 °C and freeze dried at −110 °C, 0.049 hPa (Scanvac, Denmark). PHB and glycogen extraction and analysis were done as described in Rueda et al. (2020a, 2020b). In few words, PHB was extracted by digesting 2–3 mg of freeze-dried sample in acidified MeOH and $CHCl_3$. After digestion 0.5 mL of water were added to the samples to separate solvents by density. PHB will remain in the $CHCl_3$ phase. PHB was determined by means of gas chromatography (GC) (7820A, Agilent Technologies, USA). Glycogen extraction was done by following the methodology of Lanham et al. (2012) (Lanham et al., 2012) and concentration was measured by the phenol-sulfuric acid method described in Dubois et al. (1956).

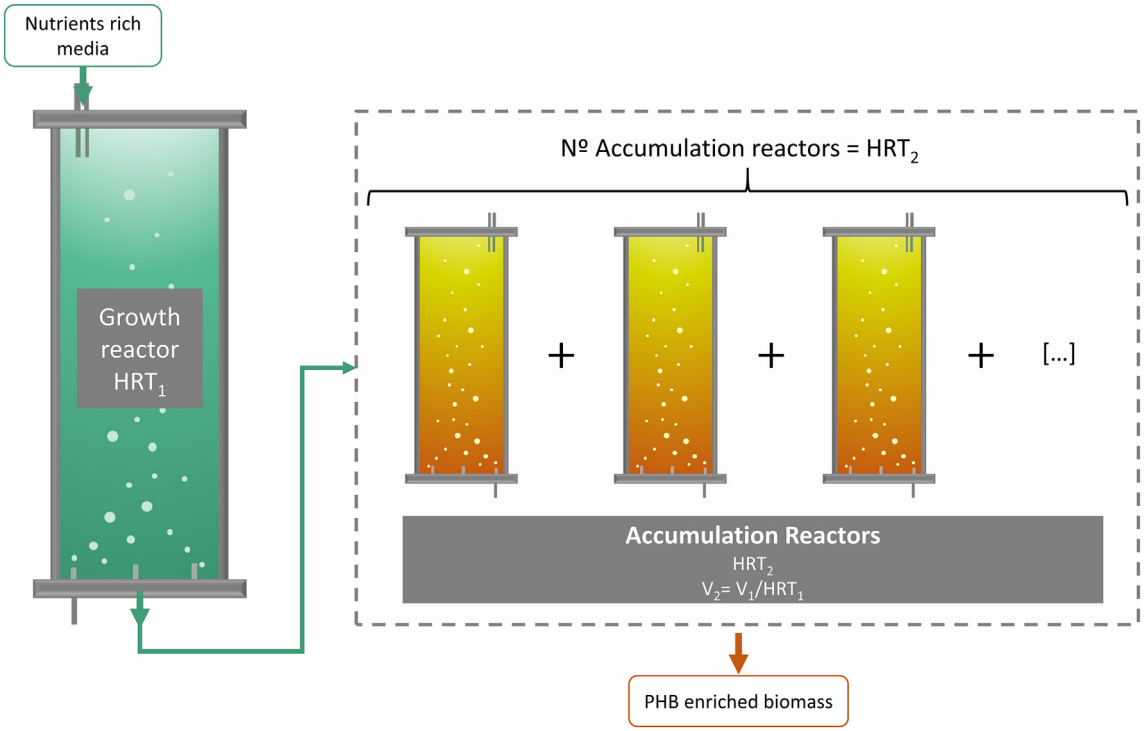

Fig. 2. Reactor configuration for the continuous production of PHB.

3. Results and discussion

3.1. Model calibration

Calibration was done by using lab scale photobioreactors inoculated with a *Synechocystis* sp. monoculture as explained in Rueda et al. (2020a, 2020b). Fig. 3 shows a comparison of experimental and simulated results, which points out that the model successfully reproduced the experimental results. Indeed, high values of r^2 and low NRMSE were observed for most of the variables (Table 3). The variables with higher correlations were NO_3^- and DIC. Results indicate that light was the variable that most limited the growth rate. Average light in the culture decreased from 20 to 5 μmol photons·m^{-2}·s^{-1} (Fig. 3.H). The calibrated half saturation constant for irradiance was 300 μmol photons·m^{-2}·s^{-1} (Table S3), what indicates that this culture was, from the very beginning, highly limited by light. Indeed, only by the effect of light limitation, the culture was growing between a 95–98% slower than its maximum velocity. The calibrated half saturation constant for irradiance found in this study was higher than the one found by Carpine et al., 2018 (9 μmol photons·m^{-2}·s^{-1}). Nevertheless, similar values were found in other studies. For instance, Straka and Rittmann, 2017 found a half maximum light absorption coefficient of 380 μmol photons·m^{-2}·s^{-1} for Synechocystis sp. PCC 6803 growing in a 370 mL reactor and Saldarriaga et al., 2020, found a value of 368.52 μmol photons·m^{-2}·s^{-1} for a consortia of microalgae isolated from landfill leachate growing in a bubble column reactor with 9 cm diameter. These differences can be explained by different light acclimation of the cultures.

PHB was also predicted with a high accuracy (r^2 of 0.89 and a NRMSE of 19%). In the case of glycogen, although the accuracy is not really high, model predicted the general tendency of experimental results (NRMSE of 41% and r^2 of 0.36). In fact, the model reproduced the glycogen decrease during the feast-famine period to compensate the lack of DIC. More experimental research on glycogen production is needed in order to improve the accuracy of this model to predict glycogen accumulation.

If the ability to reproduce experimental data of this model is compared with the previous model, it is observed, that slightly lower r^2 values are obtained here. For instance, Carpine et al., 2018, found r^2 values higher than 0.8 in all the studied variables (almost in all the cases higher than 0.9). On the contrary in the present study, only NO_3^- and DIC consumption were predicted with r^2 higher than 0.9 (Table 3). Although r^2 is lower than in previous model, it can be reasonably considered that our model can properly predict experimental data, as r^2 is enough high in almost all the cases. It should also be noted that this is a model not based on regression analysis, so although r^2 is the most extended coefficient to determine the model prediction capacity, other variables such as the comparison of the estimated values with the observed values would be more appropriate (Von Sperling et al., 2020). Here, NRMSQE is in general low, which also demonstrates the model goodness.

Model results show that PHB photosynthetic production (process 11) was the one with higher production rate, from all PHB production processes, which indicates that DIC was the main source of carbon for the produced PHB. However, by the end of the experiment glycogen conversion to PHB (process 12), became gradually more important. In fact, by the end of the experiment 45% of the PHB was produced by means of glycogen conversion. These results indicate that glycogen conversion to PHB becomes more important as cells are kept under nutrient limitation, although DIC still remains the main source to produce PHB. Similar results have been recently found by Dutt and Srivastava, 2018, who observed, by labelling the bicarbonate added in the medium, that only a 26% of the PHB produced during starvation was generated by inorganic carbon fixation. Other authors also demonstrated the importance of glycogen conversion for the PHB production. For instance, Troschl et al., 2018 concluded that PHB in Cyanobacteria are produced in three different phases; 1) biomass production with fresh nutrients, 2) photoautotrophic production of PHB, 3) intracellular conversion of glycogen to PHB. Koch et al., 2019, demonstrated by impairing some genes related with the synthesis of glycogen, that PHB is mainly produced form the glycogen pool in order to ensure a long-term survival of

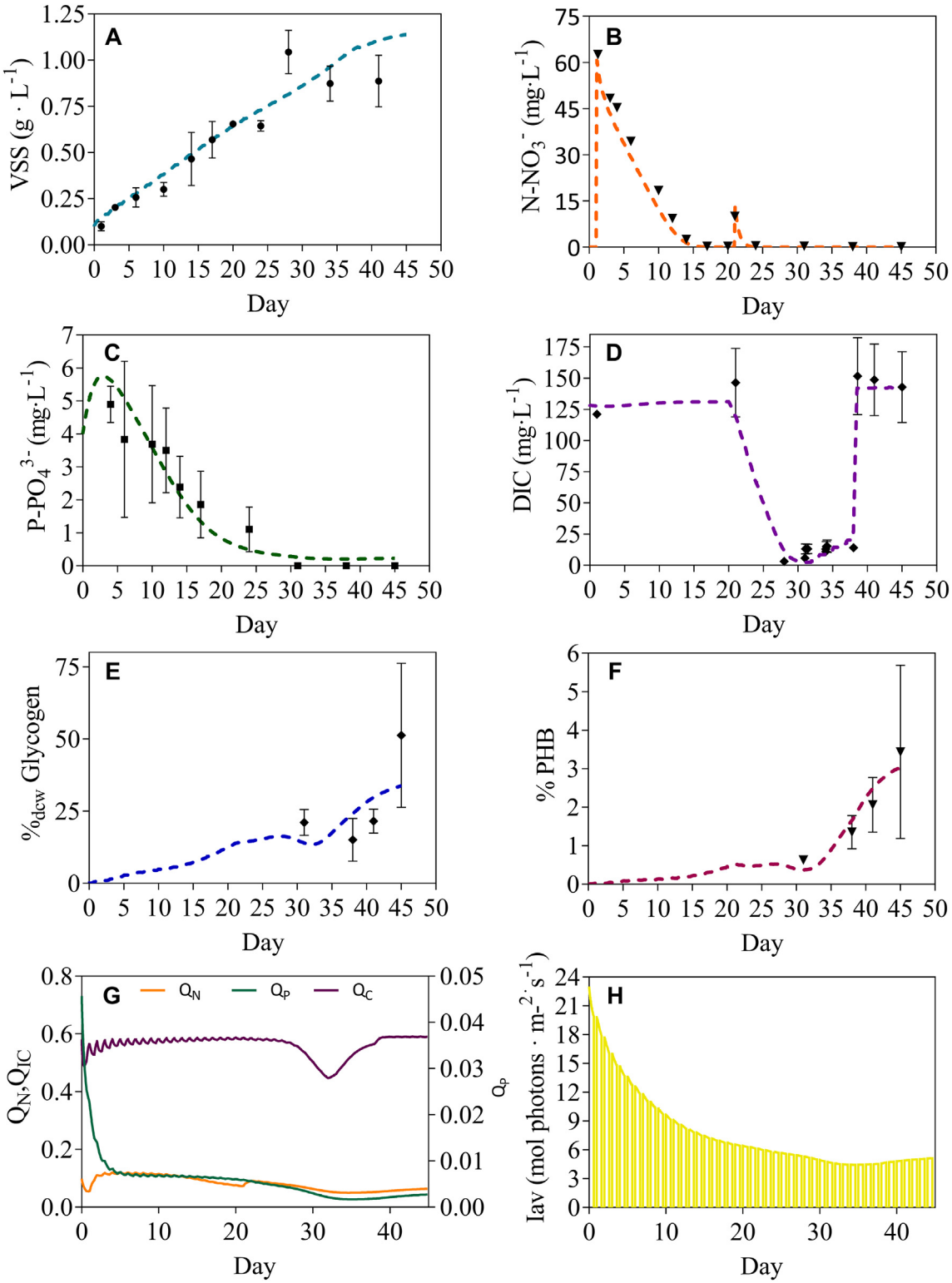

Fig. 3. Time evolution of VSS (A), NO_3^- (B), PO_4^{3-} (C), DIC (D), %glycogen (E), %PHB (F), intracellular nutrients quota (G) and average light (H). Points represent the mean value and standard deviation obtained in Rueda et al. (2020a) by two equal monocultures of *Synechocystis* sp. Lines represent the model results. These results were used for model calibration.

the cells and to prepare them for a quick response as soon as nutrients are available again. These authors found that glycogen catabolic routes that generate higher amounts of ATP while other metabolites for biosynthetic purposes are preferred for PHB synthesis (Koch et al., 2019).

3.2. Model sensitivity

Fig. 4 shows the endpoint sensitivity for VSS, glycogen and PHB. All the sensitivities were always under 15%, meaning that a change of a 20% in any of the parameters will imply a modification of VSS,

Table 3
Squared correlation coefficient (r^2) and normalized root mean square error (NRMSQE) between simulation and experimental data. Cal is calibration and Val-1 and Val-2 are the two experiments used for validation.

Data set	VSS		NO_3^-		PO_4^{3-}		DIC		PHB		Gly	
	r^2	NRMSE	r^2	NRMSE	r^2	NRMSE	r^2	NRMSE	r^2	NRMSE	r^2	NRMSE
Cal	0.87	20%	0.97	20%	0.86	27%	0.97	18%	0.89	19%	0.36	41%
Val-1	0.88	12%	0.99	3%	0.92	19%	0.93	27%	–	–	–	–
Val-2	0.62	23%	0.95	14%	0.87	23%	0.99	4%	0.57	29%	–	–

glycogen or PHB lower than a 15%. This trend suggests a high model soundness.

The parameters that most affected VSS were the cell lysis (k_{lysis}), the photosynthetic glycogen production rate (k_{C2Gly}) and the maximum % of glycogen in the cell (Gly_{max}). In the case of glycogen all the parameters had a sensitivity <10%. The photosynthetic glycogen production rate (k_{C2Gly}) and the maximum % glycogen in the cell (Gly_{max}) were the ones with a higher sensitivity. Note that the parameters related with glycogen were the ones that most affected VSS. This is related to the fact that VSS are formed by active biomass (X), glycogen and PHB. And glycogen was almost a 40% of the VSS weight, by the end of the experiment.

The parameters that most affected PHB, were photosynthetic PHB production rate (k_{C2PHB}), the nitrogen inhibition constant for PHB formation (K_{iN}^{PHB}) and the cell lysis (k_{lysis}). Results show a strong negative correlation between cellular lysis and PHB production. This is explained by the fact that a lower cellular lysis is related to a higher growth rate, which implies a higher nutrient consumption and more nutrient limitation. Results found here are in accordance with what was found by Carpine et al., 2018, which observed an adverse effect of μ_{max} in PHB production which was attributed to cellular lysis.

3.3. Model validation

Biomass (VSS) observed in the experiments used for validation was higher than in the calibration. This increase is related to light availability, which was almost 3 times the one in calibration experiments (Table 3). Despite the higher growth rate, PHB accumulated was similar to the one obtained during calibration. This is explained by the fact that during experiments done to validate this model, a higher concentration of nitrogen was added to the culture. Therefore, although cell growth and nutrients consumption rates were higher, the higher initial concentration of nutrients hindered the PHB production. These observations highlight the necessity of optimizing the initial concentrations of nutrients considering the environmental conditions.

Simulation results matched, in general, experimental data (Fig. 5). In the case of VSS (Fig. 5. A) the error of the simulations of the second validation data set was higher than in calibration (Table 3). Model underpredicted the VSS concentration during the growth phase, although similar results were reached for the stationary phase. Nutrients consumption fitted very well the experimental data sets ($r^2 > 0.87$ for PO_4^{3-} and $r^2 > 0.9$ for NO_3^- and DIC). The error of simulated PHB slightly increased with respect to the calibration results ($r^2 = 0.57$ and NRMS = 29%).

3.4. Study cases

3.4.1. Case 1: optimization of initial nutrients concentration in batch lab scale reactor for maximal PHB production

Simulation results highlight the crucial role of initial nutrient concentrations. Nevertheless, to attain a scalable process it is essential to achieve a high concentration of PHB with the minimum amount of time. For this reason, in this section optimization of the initial concentrations of N and P was done in order to attain the maximum PHB productivity. Fig. 6 shows the PHB productivity as a function of different initial concentrations of N and P. The optimal productivity was obtained at low concentration of N (between 5 and 23 $mgN \cdot L^{-1}$) and at relatively low concentration of P (between 1 and 5 $mgP \cdot L^{-1}$). Maximum

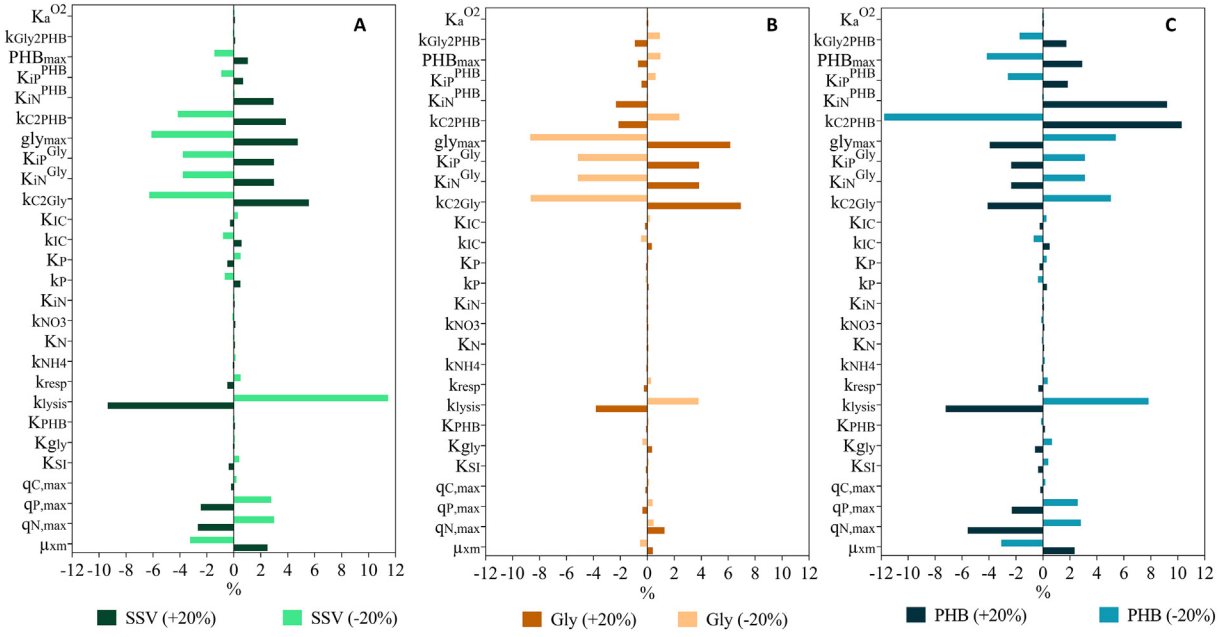

Fig. 4. Model sensitivity at the endpoint (day 45) for VSS (A), glycogen (B) and PHB (C). Light bars indicate the decrease of the parameters in a −20% and dark bars indicate the increase of the parameters in a 20%.

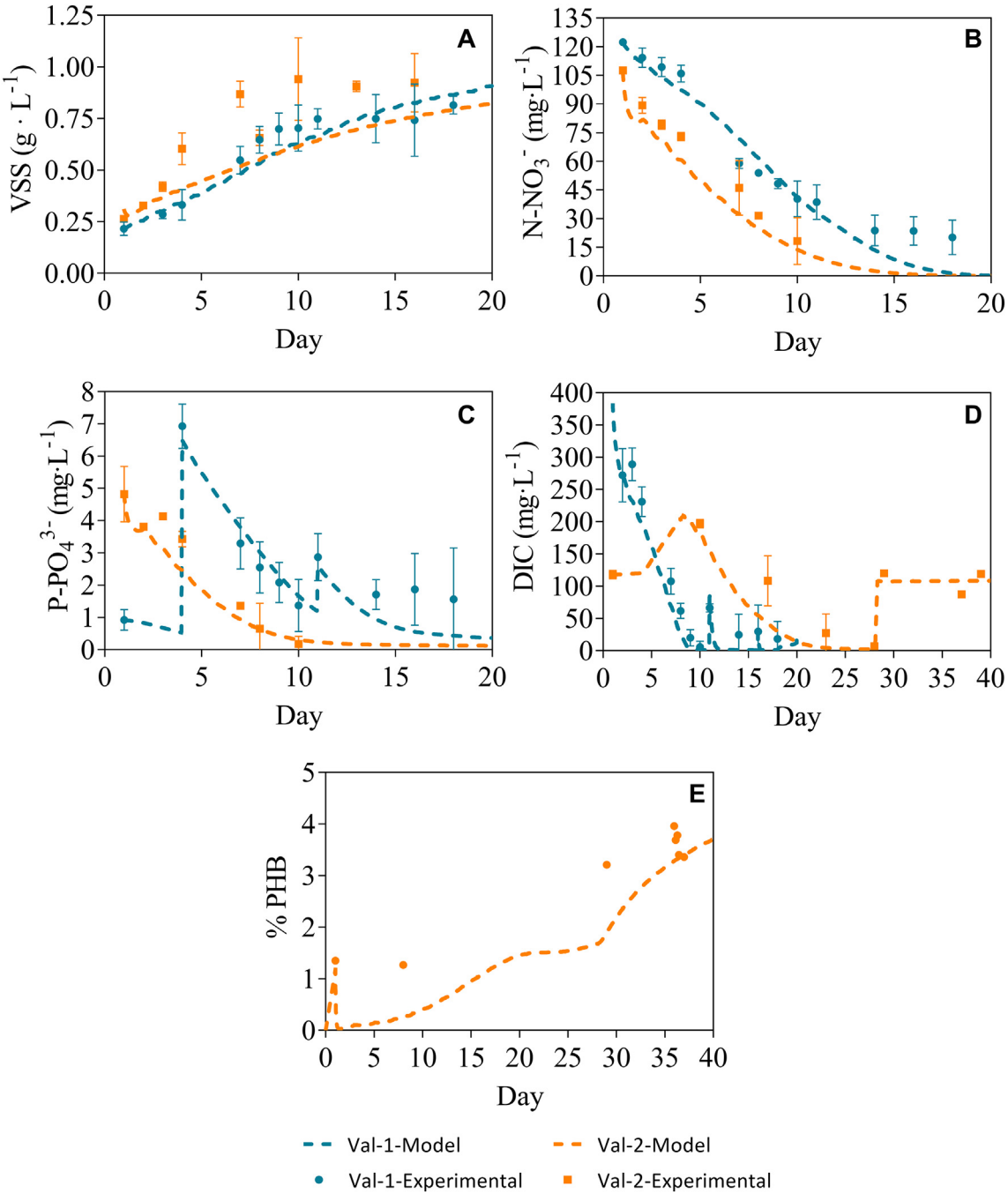

Fig. 5. Time evolution of VSS (A), NO_3^- (B), PO_4^{3-} (C), DIC (D) and % PHB. Points represent the mean value and standard deviation obtained experimentally in a monoculture of *Synechocystis* sp. Lines represent the model results. These results were used for validation.

productivity (2.3 mgPHB·L^{-1}·d^{-1}) was obtained with a N and P concentration of 6.4 mgN·L^{-1} and 2 mgP·L^{-1}, respectively. This productivity would be reached after 50 days of experiment and the PHB content would be 13.2%$_{dcw}$. Note that the optimal N:P ratio was approximately 7 (molar basis), which is lower than the Redfield ratio (N:P ratio = 15) (Redfield, 1958). These results indicate that a slight limitation of N and a moderate excess of P stimulated PHB production. This is in accordance with previous observations (Dutt and Srivastava, 2018; Kamravamanesh et al., 2019). For instance, Kamravamanesh et al., 2019 observed that P is required for glycogen synthesis. Indeed, they observed that small pulses of P boosted glycogen accumulation. On the other hand, Dutt and Srivastava, 2018 observed that PHB is mainly formed by intracellular carbon recycling. Hence, a higher initial concentration of P may cause an increase in the production of glycogen. Once P is finished, PHB will be produced from glycogen to deliver energy and NADH (Kamravamanesh et al., 2019). Regarding productivity, it should be noticed that although this optimization improved productivity from less than 0,1 mgPHB·L^{-1}·d^{-1} (experimental data), to 2.3 mgPHB·L^{-1}·d^{-1}, the productivity is still lower than the obtained in other studies. For instance, Carpine et al. (2018), obtained approximately 6,4 mgPHB·L^{-1}·d^{-1} and Kamravamanesh et al. (2017, 2018) obtained a maximum productivity of 59 mgPHB·L^{-1}·d^{-1} and 101 mgPHB·L^{-1}·d^{-1} respectively, with a wild strain. These differences can be attributed to the highest light availability of these studies, which allow them to reach higher biomass concentrations. Furthermore, strains' differences can also affect the PHB productivity.

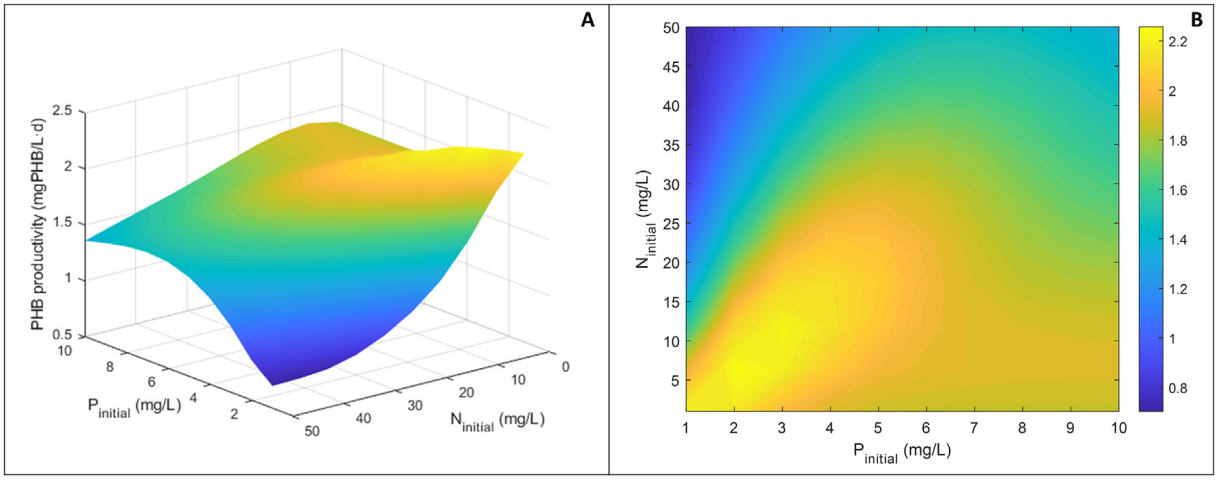

Fig. 6. Surface plot (A) and contour plot (B) of the PHB productivity related with the initial concentrations of N and P. Yellow colour represents the maximum PHB productivity and blue colour the lower. (For interpretation of colour in this figure legend, the reader is referred to the web version of this article.)

3.4.2. Case 2: optimization of continuous PHB production with Cyanobacteria

In this study, it is hypothesized that PHB could be produced continuously using reactors in series. First, a big reactor is used to grow biomass and consume nutrients. Then, the effluent of the first reactor is introduced into a set of semi-batch accumulation reactors where PHB and glycogen are accumulated. In this case study the operation conditions (nutrient loading and hydraulic retention time) of the growth reactor and the accumulation reactors are optimized to maximize PHB productivity.

Fig. 7 shows a schematic representation of the optimal operation conditions found. The optimal nutrients concentration in the influent of growth reactor were found to be 50 mgN·L^{-1} and 10 mgP·L^{-1}, and the optimal hydraulic retention time (HRT_1) was 4 days. With this HRT, nutrients were partially consumed (effluent concentrations of 15 mgN·L^{-1} and 7 mgP·L^{-1}) and 235 mgVSS·L^{-1} were achieved. The optimal HRT of the accumulation reactors was 20 days. This means that the effluent of the growing reactor (1/4 of its volume) is used to completely fill one of the 20 accumulation reactors, after 20 days this accumulation reactor is discharged and the PHB is recovered. The model predicted that with this configuration a productivity of 5.1 mgPHB·L^{-1}·d^{-1} will be achieved and an effluent with a biomass concentration of 1.4 gVSS·L^{-1} with a 9%$_{dcw}$ of PHB will be produced. Similar configurations also gave similar productivities (productivity >4 mgPHB·L^{-1}·d^{-1}, see Table S13). To achieve this high productivity HRT_1 should be between 4 and 15 days, and the HRT_2 should be between 18 and 20 days. Influent nitrogen concentration should be between 30 and 56 mgN·L^{-1} and phosphorus between 8.3 and 15 mgP·L^{-1}. More details about the best configurations obtained after the optimization can be found in Table S13. Short HRT_1 in the growth reactor and long HRT_2 in the accumulation reactors seem to be the best strategy to increase the PHB productivity. Note that a higher PHB

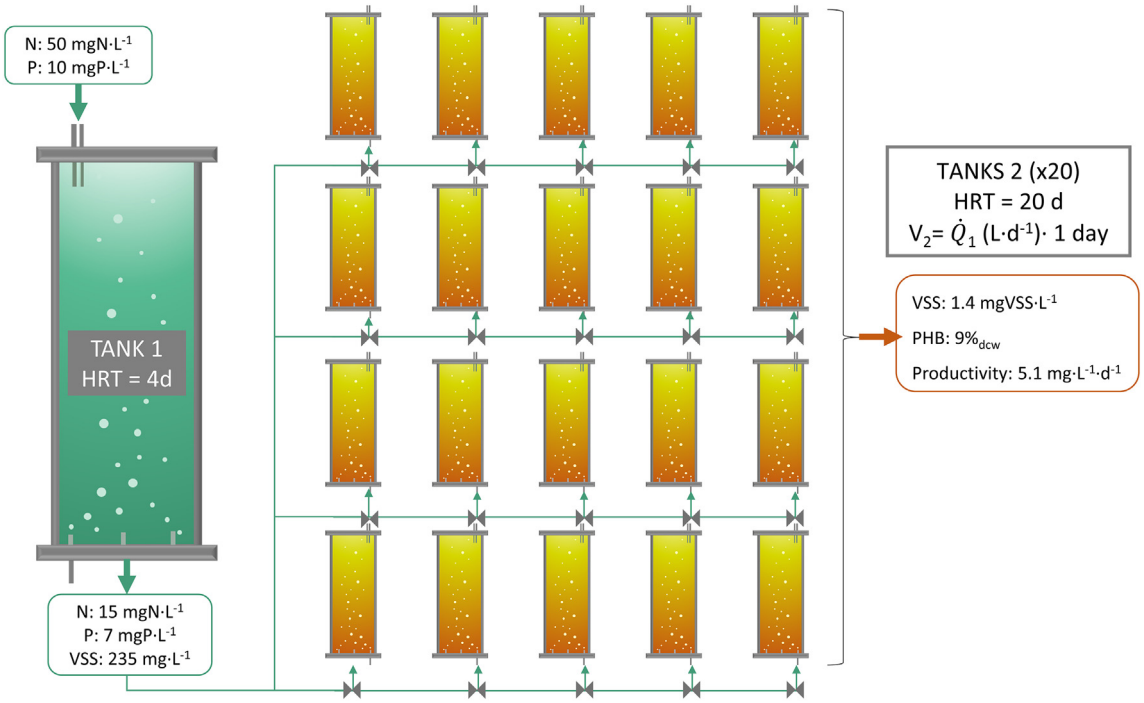

Fig. 7. Schematic representation of the optimal configuration for PHB continuous production.

concentration was obtained when larger HRT_1 were used (see Table S13). However, the higher flow rate obtained when shorter HRT_1 were applied increased the PHB productivity and compensate for the decrease in PHB concentration. Nevertheless, the downstream production costs should be considered to finally decide which is the best PHB production strategy.

There are only few studies regarding PHB production at pilot scale and with continuous reactors, which hinders the discussion of these results (Yashavanth et al., 2021). Troschl et al. (2018) found a maximum productivity of 8.5 $mgPHB \cdot L^{-1} \cdot d^{-1}$, in a 200 L tubular pilot reactor operated in semi-continuous conditions. A lower productivity was obtained in previous author's work (0,1 $mgPHB \cdot L^{-1} \cdot d^{-1}$) in a semi-continuous demonstrative plant (3 reactors of $11m^3$ each) fed with agricultural run-off and with a mixed Cyanobacteria dominated culture (Rueda et al., 2020b). Results found in this work, are within the same magnitude that the ones found by Troschl et al. (2018) and 50 times higher than the ones previously found by the authors (Rueda et al., 2020b). Different productivities may be obtained with different strains, thus, the model should be calibrated for each individual strain, what can be done using laboratory scale results for each individual case. Therefore, this model can serve as a tool to optimize industrial scale production before scaling up. Furthermore, it allows trying different reactor configurations, which may help in the decision-making process.

4. Conclusions

In this study PHB and glycogen photosynthetic production processes were studied and optimized by using a new kinetic model tool. The model was successfully calibrated and validated for a monoculture of *Synechocystis* sp. (r^2 between 0.6 and 0.99). It was also observed that the parameters that most affected PHB production were cell lysis and nitrogen inhibition constants. During model validation, it was observed that although cell growth and nutrients consumption rates were higher due to higher light intensity than in calibration experiments, the higher initial concentration of nutrients hindered the PHB production. These highlight the importance to optimize reactor operation conditions considering environmental factors. The developed model was used to optimize the initial nutrients concentration for a one-step laboratory reactor, which were found to be 6.4 $mgN \cdot L^{-1}$ and 2 $mgP \cdot L^{-1}$. Furthermore, a new reactor configuration to produce PHB in a continuous industrial scale was proposed. The optimal operation conditions for this configuration were found to be a hydraulic retention time of 4 days in the growth reactor, and a hydraulic retention time of 20 days in the accumulation reactors. Optimal nutrients concentration at growth reactor influent were 50 $mgN \cdot L^{-1}$ and 10 $mgP \cdot L^{-1}$. With this configuration a productivity of 5.1 $mgPHB \cdot L^{-1} \cdot d^{-1}$ was achieved.

The model presented in this study improves previous model about PHB production with Cyanobacteria, creating a more generalist tool, useful for any environmental condition and growth media. Moreover, this model introduces the most recent discoveries about PHB production with Cyanobacteria, such as the relevance of glycogen to produce PHB.

Considering the environmental pollution problems generated by the use of conventional plastics, new biodegradable materials produced with a low environmental impact are essential. However, biological processes need for the cleaner production of this bioplastics are complex, and usually difficult to optimize and scale up. The proposed model is as a useful tool to increase PHB productivity and successfully design and scale up PHB production with Cyanobacteria under different environmental situations and reactor configurations.

CRediT authorship contribution statement

Estel Rueda: Methodology, Validation, Software, Formal analysis, Investigation, Writing – original draft, Visualization. **Joan García:** Conceptualization, Resources, Writing – original draft, Writing – review & editing, Supervision, Project administration, Funding acquisition.

Declaration of competing interest

The authors declare that they have no known competing financial interests or personal relationships that could have appeared to influence the work reported in this paper.

Acknowledgements

This work was supported by the Spanish Ministry of Science, Innovation and Universities (MCIU), the Research National Agency (AEI), and the European Regional Development Fund (FEDER) [AL4BIO, RTI2018-099495-B-C21]. Estel Rueda would like to thank the Spanish Ministry of Education, Culture and Sports (FPU18/04941) for her grant. Authors would like to thank Professors Joan Dosta, Monica Reig i Amat and Xanel Vecino Bello for his support on pH calculations.

Appendix A. Supplementary data

Supplementary data to this article can be found online at https://doi.org/10.1016/j.scitotenv.2021.149561.

References

Abed, R.M.M., Dobretsov, S., Sudesh, K., 2009. Applications of cyanobacteria in biotechnology. J. Appl. Microbiol. 106, 1–12.
APHA, AWWA, WEF, 2012. Standard methods for the examination of water and wastewater. Stand. Methods 541.
Arias, D.M., Uggetti, E., García-Galán, M.J., García, J., 2018. Production of polyhydroxybutyrates and carbohydrates in a mixed cyanobacterial culture: effect of nutrients limitation and photoperiods. New Biotechnol. 42, 1–11.
Arias, D.M., García, J., Uggetti, E., 2020. Production of polymers by cyanobacteria grown in wastewater: current status, challenges and future perspectives. New Biotechnol. 55, 46–57.
Bekirogullari, M., Pittman, J.K., Theodoropoulos, C., 2018. Multi-factor kinetic modelling of microalgal biomass cultivation for optimised lipid production. Bioresour. Technol. 269, 417–425.
Bougaran, G., Bernard, O., Sciandra, A., 2010. Modeling continuous cultures of microalgae colimited by nitrogen and phosphorus. J. Theor. Biol. 265, 443–454.
Brun, R., Kühni, M., Siegrist, H., Gujer, W., Reichert, P., 2002. Practical identifiability of ASM2d parameters - systematic selection and tuning of parameter subsets. Water Res. 36, 4113–4127.
Carpine, R., Raganati, F., Olivieri, G., Hellingwerf, K., Pollio, A., Salatino, P., Marzocchella, A., 2018. Poly-ß-hydroxybutyrate (PHB) production by synechocystis PCC6803 from Co2. model development (2018).pdf. Algal Res. 29, 46–60.
Carpine, R., Olivieri, G., Hellingwerf, K.J., Pollio, A., Marzocchella, A., 2020. Industrial production of poly-ß-hydroxybutyrate from CO2: can cyanobacteria meet this challenge? Processes 8, 1–23. https://doi.org/10.3390/pr8030323.
Carucci, A., Dionisi, D., Majone, M, Rolle, E., Smurra, P., 2001. Aerobic storage by activated sludge on real wastewater. Water Res. 35 (16), 3833–3844.
Costa, S.S., Miranda, A.L., de Morais, M.G., Costa, J.A.V., Druzian, J.I., 2019. Microalgae as source of polyhydroxyalkanoates (PHAs) — a review. Int. J. Biol. Macromol. 131, 536–547.
Dosta Parras, J., 2007. Operation and Model Description of Advanced Biological Nitrogen Removal Treatments of Highly Ammonium Loaded Wastewaters.
Droop, R.M., 1973. Some thoughts on nutrient limitation in algae. J. Phycol. 9, 264–272.
Drosg, B., Fritz, I., Gattermayr, F., Silvestrini, L., 2015. Photo-autotrophic production of poly (hydroxyalkanoates) in cyanobacteria. Chem. Biochem. Eng. Q. 29, 145–156.
Dubois, M., Gilles, K.A., Hamilton, J.K., 1956. Colorimetric method for determination of sugars and related substances. Anal. Chem. 28, 350–356.
Dutt, V., Srivastava, S., 2018. Novel quantitative insights into carbon sources for synthesis of poly hydroxybutyrate in synechocystis PCC 6803. Photosynth. Res. 136, 303–314.
Gujer, W., Henze, M., Mino, T., Van Loosdrecht, M., 1999. Activated sludge model no. 3. Water Sci. Technol. 39, 183–193.
Kamravamanesh, D., Pflügl, S., Nischkauer, W., Limbeck, A., Lackner, M., Herwig, C., 2017. Photosynthetic poly-ß-hydroxybutyrate accumulation in unicellular cyanobacterium Synechocystis sp. PCC 6714. AMB Express, 7 https://doi.org/10.1186/s13568-017-0443-9.
Kaelin, David, Manser, Reto, Rieger, Leiv, Eugster, Jack, Rottermann, Karin, Siegrist, Hansruedi, 2009. Extension of ASM3 for two-step nitrification and denitrification and its calibration and validation with batch tests and pilot scale data. Water Research 43 (6), 1680–1692.
Kamravamanesh, D., Kovacs, T., Pflügl, S., Druzhinina, I., Kroll, P., Lackner, M., Herwig, C., 2018. Increased poly-?-hydroxybutyrate production from carbon dioxide in randomly mutated cells of cyanobacterial strain synechocystis sp. PCC 6714: mutant generation and characterization. Bioresour. Technol. 266, 34–44.

Kamravamanesh, D., Slouka, C., Limbeck, A., Lackner, M., Herwig, C., 2019. Increased carbohydrate production from carbon dioxide in randomly mutated cells of cyanobacterial strain synechocystis sp. PCC 6714: bioprocess understanding and evaluation of productivities. Bioresour. Technol. 273, 277–287.

Koch, M., Doello, S., Gutekunst, K., Forchhammer, K., 2019. PHB is produced from glycogen turn-over during nitrogen starvation in synechocystis sp. PCC 6803. Int. J. Mol. Sci. 20.

Lai, Song Yi, Kuo, Po Chih, Wu, Wei, Jang, Ming Feng, Chou, Yi Shyong, 2013. Biopolymer production in a fed-batch reactor using optimal feeding strategies. J. Chem. Technol. Biotechnol. 88 (11), 2054–2061.

Lanham, A.B., Ricardo, A.R., Coma, M., Fradinho, J., Carvalheira, M., Oehmen, A., Carvalho, G., Reis, M.A.M., 2012. Optimisation of glycogen quantification in mixed microbial cultures. Bioresour. Technol. 118, 518–525.

Markou, G., Vandamme, D., Muylaert, K., 2014. Microalgal and cyanobacterial cultivation: the supply of nutrients. Water Res. 65, 186–202.

Mulchandani, A., Luong, J.H.T., Groom, C., 1989. Substrate inhibition kinetics for microbial growth and synthesis of poly-β-hydroxybutyric acid by Alcaligenes eutrophus ATCC 17697. Appl. Microbiol. Biotechnol. 30 (1), 11–17.

Redfield, A.C., 1958. The biological control of chemical factors in the environment. Am. Sci. 46, 205–221.

Rueda, E., García-Galán, M.J., Díez-Montero, R., Vila, J., Grifoll, M., García, J., 2020a. Polyhydroxybutyrate and glycogen production in photobioreactors inoculated with wastewater borne cyanobacteria monocultures. Bioresour. Technol. 295, 122233.

Rueda, E., García-Galán, M.J., Ortiz, A., Uggetti, E., Carretero, J., García, J., Díez-Montero, R., 2020b. Bioremediation of agricultural runoff and biopolymers production from cyanobacteria cultured in demonstrative full-scale photobioreactors. Process Saf. Environ. Prot. 139, 241–250. https://doi.org/10.1016/j.psep.2020.03.035.

Ryu, K.H., Sung, M.G., Kim, B., Heo, S., Chang, Y.K., Lee, J.H., 2018. A mathematical model of intracellular behavior of microalgae for predicting growth and intracellular components syntheses under nutrient-replete and -deplete conditions. Biotechnol. Bioeng. 115, 2441–2455.

Saldarriaga, L.F., Almenglo, F., Ramírez, M., Cantero, D., 2020. Kinetic characterization and modeling of a microalgae consortium isolated from landfill leachate under a high CO2 concentration in a bubble column photobioreactor. Electron. J. Biotechnol. 44, 47–57. https://doi.org/10.1016/j.ejbt.2020.01.006.

Solimeno, A., Parker, L., Lundquist, T., García, J., 2017. Integral microalgae-bacteria model (BIO_ALGAE): application to wastewater high rate algal ponds. Sci. Total Environ. 601–602, 646–657.

Solimeno, A., Gómez-Serrano, C., Acién, F.G., 2019. BIO_ALGAE 2: improved model of microalgae and bacteria consortia for wastewater treatment. Environ. Sci. Pollut. Res. 25855–25868.

Straka, L., Rittmann, B.E., 2017. Light attenuation changes with photo-acclimation in a culture of synechocystis sp. PCC 6803. Algal Res. 21, 223–226.

Troschl, C., Meixner, K., Fritz, I., Leitner, K., Romero, A.P., Kovalcik, A., Sedlacek, P., Drosg, B., 2018. Pilot-scale production of poly-ß-hydroxybutyrate with the cyanobacterium synechocytis sp. CCALA192 in a non-sterile tubular photobioreactor. Algal Res. 34, 116–125.

Von Sperling, M., Verbyla, M.E., Oliveira, S.M.A.C., 2020. Assessment of Treatment Plant Performance and Water Quality Data: A Guide for Students, Researchers and Practitioners.

Yashavanth, P.R., Das, M., Maiti, S.K., 2021. Recent progress and challenges in cyanobacterial autotrophic production of polyhydroxybutyrate (PHB), a bioplastic. J. Environ. Chem. Eng. 9, 105379. https://doi.org/10.1016/j.jece.2021.105379.

Zhang, D., Dechatiwongse, P., Del-Rio-Chanona, E.A., Hellgardt, K., Maitland, G.C., Vassiliadis, V.S., 2015. Analysis of the cyanobacterial hydrogen photoproduction process via model identification and process simulation. Chem. Eng. Sci. 128, 130–146.

Zhang, C., Show, P.L., Ho, S.H., 2019. Progress and perspective on algal plastics – a critical review. Bioresour. Technol. 289, 121700.